Draft version June 18, 2004
Preprint typeset using LaTeX style emulateapj v. 2/19/04

PANORAMIC GALEX FUV AND NUV IMAGING OF M31 AND M33

David A. Thilker[1], Charles G. Hoopes[1], Luciana Bianchi[1], Samuel Boissier[2], R. Michael Rich[3], Mark Seibert[4], Peter G. Friedman[4], Soo-Chang Rey[4,5], Veronique Buat[6], Tom A. Barlow[4], Yong-Ik Byun[5], Jose Donas[6], Karl Forster[4], Timothy M. Heckman[7], Patrick N. Jelinsky[8], Young-Wook Lee[5], Barry F. Madore[2,9], Roger F. Malina[6], Christopher Martin[4], Bruno Milliard[6], Patrick F. Morrissey[4], Susan G. Neff[10], David Schiminovich[4], Oswald H. W. Siegmund[8], Todd Small[4], Alex S. Szalay[7], Barry Y. Welsh[8], and Ted K. Wyder[4]

Draft version June 18, 2004

ABSTRACT

We present *Galaxy Evolution Explorer* (GALEX) far-UV and near-UV mosaic observations covering the entirety of M31 and M33. For both targets, we measure the decline of surface brightness (in FUV and NUV) and changes in FUV–NUV color as a function of galactocentric radius. These UV radial profiles are compared to the distribution of ionized gas traced by Hα emission. We find that the extent of the UV emission, in both targets, is greater than the extent of the observed H II regions and diffuse ionized gas. We determine the ultraviolet diffuse fraction in M33 using our FUV observations and compare it to the Hα diffuse fraction obtained from wide-field narrow-band imaging. The FUV diffuse fraction appears to be remarkably constant near 0.65 over a large range in galactocentric radius, with departures to higher values in circumnuclear regions and, most notably, at the limit of the Hα disk. We suggest that the increase in FUV diffuse fraction at large galactocentric radii could indicate that a substantial portion of the diffuse emission beyond this point is not generated in situ but rather scattered from dust, after originating in the vicinity of the disk's outermost H II regions. Radial variation of the Hα diffuse fraction was also measured. We found the Hα diffuse fraction generally near 0.4 but rising toward the galaxy center, up to 0.6. We made no attempt to correct our diffuse fraction measurements for position-dependent extinction, so the quoted values are best interpreted as upper limits given the plausibly higher extinction for stellar clusters relative to their surroundings.

Subject headings: galaxies: individual (M31, M33) — Local Group — ultraviolet: galaxies

1. INTRODUCTION

A fundamental goal of the *Galaxy Evolution Explorer* (GALEX) mission is to gauge the history of star formation in the Universe over the interval $0 < z < 2$. This (forthcoming) analysis will depend on integrated FUV and NUV flux measurements for $> 10^7$ distant galaxies, anticipated upon completion of the GALEX imaging surveys. However, accurate interpretation of these data requires a comprehensive understanding of the possibly heterogeneous resolved UV source population amongst galaxies of diverse type. Also, detailed rest-frame UV observations of nearby galaxies are critically needed as a benchmark for optical observations of galaxy morphology at high redshift. For these reasons, in addition to the intrinsic interest in bright, well-resolved targets, the GALEX Nearby Galaxy Survey (NGS: Bianchi et al. 2004a, b) is being undertaken.

We have obtained FUV and NUV GALEX NGS observations of M31 and M33, covering the full extent of each galaxy. Local Group objects constitute an especially critical portion of the NGS sample, as our angular resolution affords separation of individual young stellar clusters from their neighbors and host environment. Furthermore, these nearby targets provide an excellent opportunity to measure properties of the apparently diffuse UV emission, uncontaminated by embedded stellar clusters which ultimately generate the extended radiation field (although some "diffuse" emission may also originate from faint, unresolved stars).

In this Letter, we describe preliminary analysis of the GALEX M31 and M33 mosaics. We characterize the overall UV morphology and contrast the GALEX sources with corresponding ionized nebulae (H II regions, shells, filaments, and diffuse gas). For reference, Keel (2000) provides a succinct review of previous UV investigations in M31 and M33.

2. OBSERVATIONS AND DATA ANALYSIS

We analyzed FUV (1350–1750 Å) and NUV (1750–2750 Å) imaging data from GALEX, plus pre-existing ground-based Hα observations. For Local Group targets

[1] Center for Astrophysical Sciences, The Johns Hopkins University, 3400 N. Charles St., Baltimore, MD 21218, dthilker,choopes,bianchi@pha.jhu.edu
[2] Observatories of the Carnegie Institution of Washington, 813 Santa Barbara St., Pasadena, CA 91101, boissier@ociw.edu, barry@ipac.caltech.edu
[3] Department of Physics and Astronomy, University of California, Los Angeles, CA 90095, rmr@astro.ucla.edu
[4] California Institute of Technology, MC 405-47, 1200 East California Boulevard, Pasadena, CA 91125, mseibert,friedman,screy,krl,cmartin,patrick,ds,tas,wyder@srl.caltech.edu, tab@ipac.caltech.edu
[5] Center for Space Astrophysics, Yonsei University, Seoul 120-749, Korea, byun@obs.yonsei.ac.kr, ywlee@csa.yonsei.ac.kr
[6] Laboratoire d'Astrophysique de Marseille, BP 8, Traverse du Siphon, 13376 Marseille Cedex 12, France, veronique.buat,jose.donas,roger.malina,bruno.milliard@oamp.fr
[7] Department of Physics and Astronomy, The Johns Hopkins University, Homewood Campus, Baltimore, MD 21218, heckman,szalay@pha.jhu.edu
[8] Space Sciences Laboratory, University of California at Berkeley, 601 Campbell Hall, Berkeley, CA 94720, patj,ossy,bwelsh@ssl.berkeley.edu
[9] NASA/IPAC Extragalactic Database, California Inst. of Tech., Mail Code 100-22, 770 S. Wilson Ave., Pasadena, CA 91125
[10] Laboratory for Astronomy and Solar Physics, NASA GSFC, Greenbelt, MD 20771, neff@stars.gsfc.nasa.gov

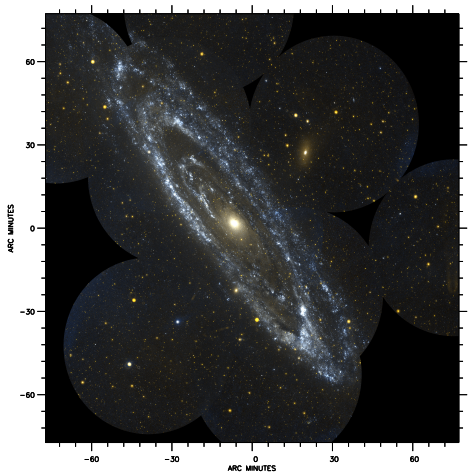

FIG. 1.— The centermost $3 \times 3°$ region of the GALEX M31 mosaic. The image, a composite representation of our FUV and NUV data, has been created so as to make sources brightest in FUV appear blue and those features brightest in NUV appear orange. Regions which are especially bright in both bands are rendered nearly white. Note that two of the early "test" pointings listed in Table 1 (M31-F1, M31-F3) and depicted here lie within the bright disk of the galaxy, where they were reimaged with the subsequent grid of "mosaic" fields. Six of the 15 M31 fields do not appear in this image (MOS1,5,6,9,10,11) as they are located outside the bounds of the figure. The conspicuous gap in coverage to the SW of Andromeda's southern tip is caused by the need to avoid a bright field star. Later in the GALEX mission, the bright star limit will be relaxed. When this takes place, we will observe the M31 coverage gaps as much as practical.

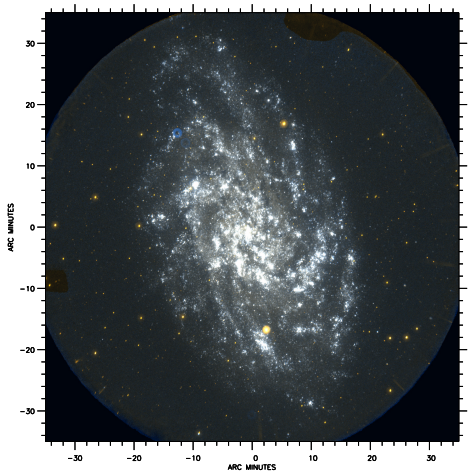

FIG. 2.— The central field of the M33 GALEX mosaic. The color-composite image has been created as for M31 in Fig. 1, with FUV-bright regions appearing blue. A contiguous area extending $\sim 2.6°$ in diameter around M33 has already been observed.

within the NGS, the GALEX mission plan calls for two integrations (conducted during separate orbits), amounting to a total of $\sim$ 3 ks per field. The imagery presented here represents most of the eventual M31/M33 database, but one pointing in M33 and a few in M31 remain to be observed for the second time. We note that fields probing some portions of Andromeda's extreme outer HI disk and high-velocity cloud population (Thilker et al. 2004, Braun et al. in prep) are not yet available.

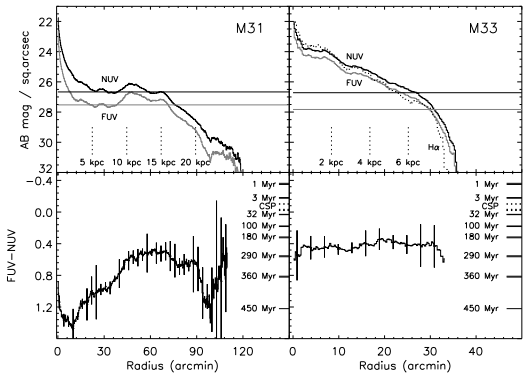

FIG. 3.— Radial profiles of FUV, NUV surface brightness and FUV–NUV color in M31 and M33. On the top panels of the figure we plot the median surface brightness (AB mag / sq. arcsec) in both bands. The dark line indicates NUV, whereas the light colored line shows FUV. We also plot the estimated sky background with horizontal lines. An Hα profile for M33 is also plotted, with the normalization adjusted to match the FUV at $30'$ radius. Note the remarkable range in surface brightness probed from the inner disk to the outer disk. For this measurement, we took the median value within each concentric elliptical annulus so as to gauge the "background" underlying stellar population, rather than the (luminosity-weighted) mean which is biased toward the clusters which are presently UV-brightest. The bottom panels show median FUV–NUV with error bars ($\pm 1\sigma$) indicated on the profile. We also plot intrinsic and reddened synthetic colors for instantaneous burst populations of varied age and three prolonged periods of continuous star formation (CSP: 100 Myr, 1 Gyr, 10 Gyr). In M31, note the strong FUV–NUV indication for rather minimal recent SF (during the past 500 Myr) within the interarm gap between Andromeda's bulge and 5 kpc arm. Our measurements have not been corrected for the variable extinction which is bound to exist.

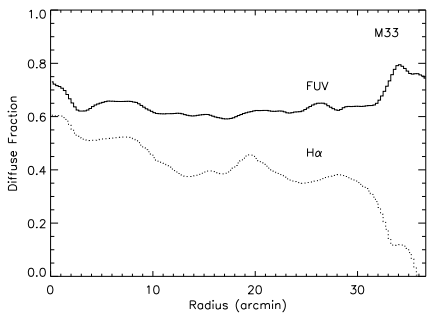

FIG. 4.— The diffuse fraction in FUV and Hα as a function of galactocentric radius in M33. The effective resolution of these curves is $\sim 400''$, owing to the method used to isolate the DIG from compact sources.

The tiling of M31, which incorporates some coverage gaps, was dictated by the need to avoid bright stars. Fifteen 1.25° diameter fields were observed. Central coordinates and total exposure times are given in Table 1. M33 has been surveyed in its entirety without any gaps, using one "first-look" exposure of the northern disk and a 7-pointing hexagonal mosaic centered on the galaxy. The majority of M33 lies within the central pointing of this mosaic. Figures 1 and 2 present our GALEX (FUV, NUV) color-composite images of M31 and M33.

For M31, we compared the GALEX observations with Hα data from 10 KPNO-4m/MOS fields belonging to the NOAO "Survey of Local Group Galaxies Currently

TABLE 1
GALEX FIELDS FOR M31 AND M33

Field	α_{J2000}	δ_{J2000}	Exp. (s)
M31-F1	00:42:37.01	41:13:22.08	650
M31-F3	00:45:00.00	41:51:24.84	1704
M31-MOS0	00:40:40.11	40:49:57.25	2437
M31-MOS1	00:35:30.52	41:05:53.34	2180
M31-MOS2	00:39:24.06	41:51:18.50	1637
M31-MOS3	00:45:34.56	40:32:05.78	2374
M31-MOS4	00:44:46.35	41:32:38.22	2750
M31-MOS5	00:33:25.82	39:57:06.66	1642
M31-MOS6	00:45:11.80	39:34:21.00	3075
M31-MOS7	00:43:33.38	42:34:07.90	2762
M31-MOS8	00:48:40.83	42:01:58.15	2699
M31-MOS9	00:36:26.40	42:45:00.72	3265
M31-MOS10	00:29:42.56	40:44:45.92	1452
M31-MOS11	00:48:51.16	42:57:45.14	1879
M31-MOS12	00:41:23.84	40:21:34.52	3031
M33	01:33:52.27	31:08:19.61	1660
M33-MOS0	01:33:50.90	30:39:36.00	3399
M33-MOS1	01:31:53.70	31:22:50.02	3409
M33-MOS2	01:29:58.40	30:39:22.00	3366
M33-MOS3	01:31:55.60	29:56:13.99	1959
M33-MOS4	01:35:46.30	29:56:15.00	3269
M33-MOS5	01:37:43.40	30:39:24.01	3035
M33-MOS6	01:35:48.00	31:22:50.99	3171

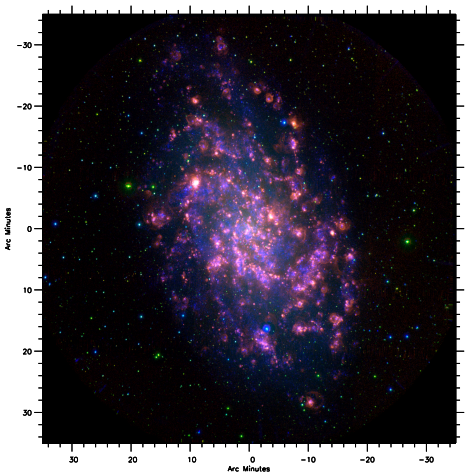

FIG. 5.— Multi-wavelength view of M33, showing the same field as Fig. 2 (11.4 kpc in projected extent). The color channels of this image are assigned as follows: Hα + continuum (red), continuum (green), GALEX NUV (blue). Differences in overall NUV and Hα morphology highlight the advantage of UV observations as a direct tracer of sites which have recently hosted star-formation, rather than the environmentally dependent, indirect, and highly age-sensitive view given by Hα. This is not meant to downplay the importance of Hα observations, but rather to highlight the importance of both datasets whenever the goal is to obtain a comprehensive view of star-formation over the past few hundred Myr.

Forming Stars" (Massey et al. 2001). In M33, we used a Burrell Schmidt Hα mosaic (Hoopes & Walterbos 2000) covering all of the disk.

We adopt distances of 770 and 840 kpc, respectively, to M31 and M33 (M31: Freedman & Madore 1990, M33: Freedman, Wilson, & Madore 1991). The 5″ FWHM GALEX PSF corresponds to $\sim$ 20 pc. RMS flux sensitivity varies with position. Typical 1σ limits are 6.6 and 2.8×10^{-19} erg s^{-1} cm^{-2} Å^{-1} for FUV and NUV, respectively, evaluated at the scale of the PSF. Expressed in terms of surface brightness, these limits correspond to

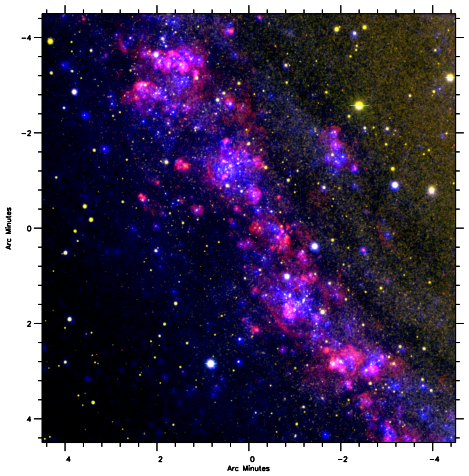

FIG. 6.— A small section of M31's spiral arm structure, located to the NE of the galaxy center. The color channels of this image are assigned as follows: Hα + continuum (red), continuum (green), GALEX NUV (blue). The detected distribution of NUV sources is clearly more extensive than observed in Hα, whereas the morphology of emission line structures can provide valuable information on the radiative- and mechanically-driven ISM feedback processes associated with massive stars.

28.0(28.2) AB mag arcsec^{-2} in FUV(NUV). This sensitivity is sufficent to detect substantial diffuse emission throughout both galaxies.

3. UV MORPHOLOGY AND CORRELATION WITH Hα

Figure 3 presents FUV, NUV, and FUV–NUV radial profiles for both galaxies. For M33, we also show a radial profile for diffuse Hα emission. We have measured the median (sky-background-subtracted) surface brightness in concentric elliptical annuli to 2° along the major axis for M31 and 0.6° for M33, stepping by 15″. A complete description of the procedure is given by Bianchi et al. (this volume). In M31, to the limit of our sensitivity, there is no well-defined "edge" of the stellar disk traced by the GALEX observations. At least out a galactocentric distance of 27 kpc, there is no significant downturn in the surface density of intermediate mass stars producing the observed UV radiation in M31. This is interesting given the much more obvious limit to the extent of H II regions traced in Hα imaging ($\sim$ 20 kpc). Enhancements in the median surface brightness occur at radii dominated by Andromeda's well-known 10 and 15 kpc arms. In M33, at the disk's edge, we note that the UV emission drops off significantly slower than the median Hα emission. Furthermore, we see no evidence for a UV edge at 32' reported by Buat (1994), most likely a consequence of our improved sensitivity. On both FUV–NUV panels, we indicate Bruzual & Charlot (2003) model colors for starbursts spanning a range in age, and three model colors appropriate for differing periods of continuous star formation. The plotted models are for solar metallicity. When interpreting the measured colors in relation to the starburst models, one may consider the age corresponding to the best matching model color as the age of the last major star formation episode. In both galaxies, the FUV–NUV color of the typical stellar population generally becomes bluer with increasing radius, however the magnitude of this effect is variable. In M33, the outward trend toward bluer UV color is slight and FUV–NUV

remains remarkably constant over the majority of the galactocentric radii examined. This reflects the global extent of recent star formation in M33. Almost every locale within M33 has undergone a significant burst within the past $\sim$ 200 Myr. See Bianchi et al. (this volume) for similar analysis of M51 and M101.

The proximity of our Local Group targets provides an excellent opportunity for decomposition of the GALEX imaging data into discrete (compact) sources and diffuse emission, especially so for M33 due to its favorable inclination ($i = 57°$). As in the study of diffuse ionized gas (DIG, Hoopes et al. 2001), the UV diffuse fraction (defined as the integral of diffuse emission / integral of all emission) can be used to consider issues of radiation transport in the ISM. The UV diffuse fraction acts as a indicator for the origin and subsequent path of non-ionizing photons, whereas the Hα diffuse fraction provides an indirect tracer of the Lyman continuum.

We measured the diffuse fraction (in FUV, NUV, and Hα) as a function of radius in M33 using our GALEX data and the Schmidt mosaic of Greenawalt (1998). This was accomplished by computing the average ratio of two images in elliptical annuli oriented to match the M33 disk. The first of these two images was a representation of the diffuse emission on 1.5 kpc scales, generated by applying a large circular median-filter to the data. The median operator effectively eliminated the flux from all discrete structures smaller than 1.5 kpc. The second image contributing to our measured ratio was a smoothed version of the original data, generated by convolving with a Gaussian kernel sized to achieve resolution (1.5 kpc) matching the median image described above. Both these images were background subtracted before computation of the diffuse fraction. To verify the accuracy of our method in the UV, we compared with published work on the diffuse ionized gas. Consistent with Hoopes & Walterbos (2000), we find that the Hα diffuse fraction is approximately 0.4 at radii hosting the bulk of M33's emission line gas. We determined the UV diffuse fraction in M33 using both FUV and NUV images, but found the NUV estimate is notably contaminated (in spots) by foreground stars. Accordingly, we adopt the FUV-band for gauging the UV diffuse fraction.

Figure 4 presents the UV and Hα diffuse fractions measured for M33. The ultraviolet diffuse fraction appears to be remarkably constant near 0.65 over a large range in galactocentric radius, with departures to higher values in circumnuclear regions and, most notably, at the limit of the Hα disk. The increase in FUV diffuse fraction at large galactocentric radii may reflect that a substantial portion of the diffuse emission beyond this point is not generated in situ but rather scattered from dust, after originating in the vicinity of the disk's outermost H II regions. Note that we have not attempted correction of the UV diffuse fraction for decreased extinction in the field away from compact star forming regions, but it is possible that the UV diffuse fraction could adjust substantially downward once this is considered (Buat et al. 1994). Radial variation of the Hα diffuse fraction was also measured. We found values generally near 0.4 but rising toward the galaxy center, up to 0.6.

The relative intensity of diffuse UV and Hα emission and UV color in DIG as a function of distance from associated stellar clusters is another useful probe of the ISM. Indeed, the ionization mechanism of the DIG has long been a puzzle, as it requires a very large (30-50% of the ionizing photons from a galaxy's OB stellar pop.), sustained energy source for the gas to remain ionized. If OB stars in cluster environments are responsible for the ionization, the Lyman continuum photons must "leak" from H II regions. Hoopes & Walterbos (2000) first considered the contribution of field OB stars as an additional way to support the DIG, finding that they can account for roughly 40% of the observed emission. Our GALEX observations will soon be used to measure extinction corrected FUV/Hα and FUV–NUV within the DIG, comparing FIR, NIR bands with our FUV image to gauge extinction (Thilker et al. in prep.).

The GALEX FUV and NUV imagery of M31 and M33 allows for a detailed study of the relation between resolved emission line structures (traced by Hα) and young stellar clusters (and/or single massive stars). For this Letter, we present an overview of the issue. Figure 5 shows a color-composite image of Hα + continuum (red), continuum (green), and GALEX NUV (blue) imagery for the whole of M33, whereas Fig. 6 presents an analogous high-resolution view for a spiral arm segment in M31. [Note that the full-quality figures of this paper are electronically available, and retain much more detail than in print.] The GALEX imagery exhibits nearly one to one correlation with the distribution of H II regions (as expected), but notably also shows UV bright clusters or star inside the vast majority of apparent Hα bubbles. Although Hα is a very sensitive tracer of massive star formation, it reveals only those sources which are still very young. GALEX provides a more complete census of recent star formation as it traces young-to-moderate age stellar populations, up to several hundred Myr, unless they are highly obscured. This conclusion is obvious from inspection of Figs. 5 and 6, and serves to highlight the most basic premise of the GALEX mission: to survey cosmic star formation history in the vacuum ultraviolet.

GALEX (Galaxy Evolution Explorer) is a NASA Small Explorer, launched in April 2003. We gratefully acknowledge NASA's support for construction, operation, and science analysis for the GALEX mission.

REFERENCES

Bianchi, L., Madore, B., Thilker, D., Gil de Paz, A., and Martin, C., 2004a, in "The Local Group as an Astrophysical Laboratory"
Bianchi, L., Madore, B., Thilker, D., Gil de Paz, A., and the GALEX team, 2004b, AAS 203, 91.12
Bruzual, G. & Charlot, G., 2003, MNRAS, 344, 1000
Buat, V. et al. 1994, A&A, 281, 666
Freedman, W. L. & Madore, B. F. 1990, 365, 186
Freedman, W. L., Wilson, C. D., & Madore, B. F. 1991, ApJ, 372, 455
Greenawalt, B. 1998, Ph.D. thesis, New Mexico State University
Hoopes, C. G. & Walterbos, R. A. M. 2000, ApJ, 541, 597
Hoopes, C. G., Walterbos, R. A. M., Bothun, G. 2001, ApJ, 599, 878
Keel, W. C., 2000, in "The Interstellar Medium in M31 and M33, Proceedings 232. WE-Heraeus Seminar", 22-25 May 2000, Bad Honnef, Germany
Massey,P., et al. 2001, AAS 13.005
Thilker, D. A. et al. 2004, ApJ601, 39